Scattering phase shifts and mixing angles for an arbitrary number of coupled channels on the lattice

Lukas Bovermann,[1, *] Evgeny Epelbaum,[1, †] Hermann Krebs,[1, ‡] and Dean Lee[2, §]

1 Ruhr-Universität Bochum, Fakultät für Physik und Astronomie,
Institut für Theoretische Physik II, D-44780 Bochum, Germany

2 Facility for Rare Isotope Beams and Department of Physics and Astronomy, Michigan State University, MI 48824, USA

We present a lattice method for determining scattering phase shifts and mixing angles for the case of an arbitrary number of coupled channels. Previous lattice studies were restricted to mixing of up to two partial waves for scattering of two spin-1/2 particles, which is insufficient for analyzing nucleon-nucleus or nucleus-nucleus scattering processes. In the proposed method, the phase shifts and mixing angles are extracted from the radial wave functions obtained by projecting the three-dimensional lattice Hamiltonian onto the partial wave basis. We use a spherical wall potential as a boundary condition along with a channel-mixing auxiliary potential to construct the full-rank S-matrix. Our method can be applied to any type of particles, but we focus here on scattering of two spin-1 bosons involving up to four coupled channels. For a considered test potential, the phase shifts and mixing angles extracted on the lattice are shown to agree with the ones calculated by solving the Schrödinger equation in the continuum.

PACS numbers: 13.75.Cs,21.30.-x,13.85.Dz

I. INTRODUCTION

Lattice simulations provide a powerful computational approach to systems of strongly interacting particles, which is widely used in condensed matter, nuclear and particle physics. In particular, lattice gauge theory is the only known numerical method that allows one to directly solve QCD in the non-perturbative domain. Here, a remarkable progress has been achieved in the recent decades due to the rapid increase of computational power and algorithmic efficiency. In particular, high-precision lattice QCD calculations of hadronic observables such as e.g. the masses and decay constants are already available for physical values of the quark masses [1]. While hadronic reactions and resonance properties can also be addressed in lattice QCD, such calculations appear to be much more challenging and require developing reliable methods for relating the scattering amplitude to discrete finite-volume spectra accessible in lattice simulations, see [2–4] for recent work along this line and [5] for a review article.

Lattice methods have also proven to be very efficient in describing low-energy nuclear systems in the framework of chiral effective field theory (EFT). Recently, the chiral expansion of the nucleon-nucleon (NN) potential has been pushed to fifth order (N⁴LO) [6–9] within the continuum formulation. The NN potentials derived in chiral EFT in Ref. [10] allow, for the first time, for a nearly perfect description of the neutron-proton and proton-proton scattering data below the pion production threshold, which is comparable to or even better than that based on the available phenomenological potentials. Three- and four-nucleon forces have been worked out completely up to fourth order (N³LO) of the chiral expansion [11–14], see also Refs. [15–18] for the derivation of selected contributions at N⁴LO and Refs. [19–21] for review articles. To apply the interactions derived in chiral EFT to few- and many-nucleon systems, it is necessary to solve the quantum mechanical A-body problem, which can be achieved using continuum *ab initio* methods including Faddeev-Yakubovsky equations [22], the no-core configuration interaction approach [23], coupled-cluster expansions [24], the in-medium similarity renormalization group approach [25], self-consistent Green's function [26] or quantum Monte Carlo methods [27]. Alternatively, a discretized version of chiral EFT [28–30] has

---
*Email: lukas.bovermann@rub.de
†Email: evgeny.epelbaum@rub.de
‡Email: hermann.krebs@rub.de
§Email: leed@frib.msu.edu

been successfully applied to a broad range of nuclear systems. This approach has an appealing feature of being well suited for dealing with strongly clustered systems such as e.g. the famous Hoyle state in ^{12}C [31–33] and some of the low-lying states of ^{16}O, which often represent a challenge for continuum methods. See Ref. [34] for a recent review on clustering in light nuclei. So far, nuclear lattice simulations have been carried out for light and medium-mass nuclei and neutron matter up to third order in the chiral expansion [35–37]. For a recent lattice EFT study of NN scattering at N^{3}LO see Ref. [38]. This method was also employed to study the dependence of the triple-alpha process on the fundamental constants of nature [39, 40], see Ref. [41] for a related discussion, to investigate the isotopic dependence of nuclear clustering [42] and to determine the features of the nuclear force essential for nuclear binding [43]. It is important to emphasize that the development of chiral EFT interactions is more difficult on the lattice than in the continuum as it requires establishing efficient techniques for extracting the scattering amplitude from the finite-volume discrete spectra and for dealing with the breaking of rotational [44, 45] and Galilean invariance [46] due to nonzero lattice spacing. Lüscher's finite-volume method is one possible approach to compute the scattering phase shifts on the lattice. However, this method is expected to suffer from potentially large errors due to stochastic and systematic uncertainties in the energies, calculated on the lattice using Monte Carlo methods, when applied to heavier systems. In addition, it is difficult to apply for calculating partial wave mixing. For this reason, a more robust approach based on the spherical wall boundary conditions [47] was used in Refs. [38, 44, 48, 49]. This technique is not only applicable to calculations of NN phase shifts on the lattice, but can also be combined with the adiabatic projection method [50, 51], which allows one to access nuclear reactions via lattice simulations, see Ref. [52] for the first *ab initio* study of alpha-alpha scattering. However, the spherical wall method has so far only been applied to uncoupled partial waves and the cases of two coupled channels, which is insufficient for studying nuclear reactions. The purpose of this paper is to generalize this technique to an arbitrary number of coupled channels.

Our paper is organized as follows. In section II, we introduce the lattice notation, review the method of Ref. [49] to compute the scattering parameters with up to two coupled channels and extend this approach to scattering of particles or nuclear clusters of an arbitrary high spin. As an application, we consider in section III the scattering problem of two spin-1 bosons using a toy-model potential which is similar to the one from Refs. [48, 49]. The main results of our study are summarized in section IV.

II. SCATTERING OF TWO PARTICLES WITH ARBITRARY SPIN ON THE LATTICE

A. Calculational setup

We employ a periodic cubic lattice with the length L and spacing a, and define orthonormal lattice states $|\vec{r}\rangle$ with

$$r_1, r_2, r_3 = 0, \ldots, L - 1 \tag{1}$$

and

$$|\vec{r}\rangle = |\vec{r} + L\vec{e}_1\rangle = |\vec{r} + L\vec{e}_2\rangle = |\vec{r} + L\vec{e}_3\rangle \tag{2}$$

due to the periodic boundary condition. All quantities in this section are given in dimensionless lattice units, i. e. they must be multiplied by an appropriate power of the lattice spacing a to obtain their physical values. In the following, we briefly review the method to compute the scattering phase shifts and mixing angles for up to two coupled channels introduced in Ref. [49], which will then be generalized to the case of three or more coupled channels.

We consider the general scattering problem of two particles with spins s_1, s_2 and masses m_1, m_2 interacting with the potential $V(\vec{r})$. The free Hamiltonian in the center-of-mass system (CMS) is discretized as [48]

$$H_0 |\vec{r}\rangle = \frac{49}{12\mu} |\vec{r}\rangle - \frac{3}{4\mu} \sum_{i=1}^{3} (|\vec{r} + \vec{e}_i\rangle + |\vec{r} - \vec{e}_i\rangle) + \frac{3}{40\mu} \sum_{i=1}^{3} (|\vec{r} + 2\vec{e}_i\rangle + |\vec{r} - 2\vec{e}_i\rangle) \tag{3}$$

$$- \frac{1}{180\mu} \sum_{i=1}^{3} (|\vec{r} + 3\vec{e}_i\rangle + |\vec{r} - 3\vec{e}_i\rangle)$$

using the reduced mass $\mu = m_1 m_2 / (m_1 + m_2)$. The above expression corresponds to the $\mathcal{O}(a^4)$-improved free lattice Hamiltonian. To avoid artifacts induced by the periodic boundary conditions, it is convenient to use a spherical wall

boundary condition by adding the potential

$$V_{\text{wall}}(\vec{r}) = \Lambda\theta(r - R_{\text{W}}) \tag{4}$$

where θ is the Heaviside function, R_{W} is the wall radius and Λ is a large positive constant[1] [48]. Calculating the scattering parameters at low momenta usually requires large lattices which makes the analysis computationally expensive. It is more convenient to introduce an auxiliary potential outside of the range of V, which can be chosen e.g. of a Gaussian type

$$V_{\text{aux}}(\vec{r}) = V_0\, e^{-(r - R_{\text{W}})^2}\theta(R_{\text{W}} - r) \tag{5}$$

with $V_0 \leq 0$ in order to control the eigenenergies of the Hamiltonian [49]. The complete Hamiltonian including all contributions is then given by

$$H = H_0 + V + V_{\text{wall}} + V_{\text{aux}}\,. \tag{6}$$

B. Projection onto partial waves

The three-dimensional problem can be reduced to the one-dimensional one by defining radial states for a partial wave $^{2s+1}l_j$,

$$|R\rangle_{s,l,j} = \sum_{\vec{r}}\sum_{l_{\text{z}},s_{\text{z}}}\sum_{s_{1,\text{z}}}\sum_{s_{2,\text{z}}} C^{j,l,s}_{j_{\text{z}},l_{\text{z}},s_{\text{z}}} C^{s,s_1,s_2}_{s_{\text{z}},s_{1,\text{z}},s_{2,\text{z}}} Y_{l,l_{\text{z}}}(\vec{r}/r)\delta_{r,R}\,|\vec{r}\rangle \otimes |s_{1,\text{z}}, s_{2,\text{z}}\rangle\,, \tag{7}$$

i. e. the lattice sites $\vec{r}$ with the same radial distance R are grouped together according to the irreducible representations of the rotational group. Here, $C^{j,l,s}_{j_{\text{z}},l_{\text{z}},s_{\text{z}}}$ and $C^{s,s_1,s_2}_{s_{\text{z}},s_{1,\text{z}},s_{2,\text{z}}}$ are the Clebsch-Gordan coefficients for the spin-orbit and spin-spin couplings, respectively. The spherical harmonics $Y_{l,l_{\text{z}}}$ behave like $Y_{l,l_{\text{z}}}(\vec{0}) = \delta_{l,0}/\sqrt{4\pi}$ at the origin. Since the results obtained here do not depend on j_{z} in the continuum limit, we can choose $j_{\text{z}} = 0$.

Note that the radial states have to be normalized by dividing them by the square root of their norm. States that are not linearly independent or have vanishing norm must be omitted to make the norm matrix invertible. Afterwards, the Hamiltonian can be projected onto the normalized radial states. For n coupled channels with

$$|R\rangle_\alpha := |R\rangle_{s_\alpha,l_\alpha,j_\alpha}\quad\text{for }\alpha = 1,\ldots,n, \tag{8}$$

one has

$$(H_{\text{r}}(R_1, R_2))_{\alpha\beta} = \sum_{\alpha',\beta'=1}^{n} (N^{-1/2}(R_1))_{\alpha\alpha'}\;{}_{\alpha'}\langle R_1|\, H\, |R_2\rangle_{\beta'}\,(N^{-1/2}(R_2))_{\beta'\beta}\,, \tag{9}$$

where $N^{-1/2}$ is the inverse square root of the norm matrix

$$(N(R))_{\alpha\alpha'} = {}_\alpha\langle R|R\rangle_{\alpha'}\,. \tag{10}$$

Multiplying the eigenvectors of the projected Hamiltonian H_{r} by $N^{-1/2}$ from the left yields the radial wave functions

$$\psi(r) = (\psi_1(r),\ldots,\psi_n(r))^{\text{T}}\,. \tag{11}$$

---

[1] Following Ref. [49], we use the value $\Lambda = 10^6$ in the numerical calculations.

C. Single-channel case

Outside of the range of the potential, the radial wave functions are linear combinations of the spherical Hankel functions $h_l^{\pm}(pr)$, where p is the momentum in the CMS. For a single scattering channel, one obtains a wave function of the form

$$\psi(r) = Ah_l^-(pr) + Bh_l^+(pr), \tag{12}$$

which allows one to extract the phase shift δ_l from the S-matrix via

$$S = B/A = e^{2i\delta_l}. \tag{13}$$

The coefficients A, B are computed by fitting the spherical Hankel functions to the wave function in an interval $[R_{\rm I}, R_{\rm O}]$ outside of the range of the potential. The momentum p is determined from the eigenenergy of the Hamiltonian using the lattice dispersion relation

$$E(\vec{p}) = \frac{49}{12\mu} - \frac{3}{2\mu}\sum_{i=1}^{3}\cos(p_i) + \frac{3}{20\mu}\sum_{i=1}^{3}\cos(2p_i) - \frac{1}{90\mu}\sum_{i=1}^{3}\cos(3p_i). \tag{14}$$

This equation can be expressed in spherical coordinates with

$$\vec{p} = (p\sin\theta\cos\phi,\ p\sin\theta\sin\phi,\ p\cos\theta). \tag{15}$$

In order to remove the angular dependence, the dispersion relation must be projected onto partial waves as well:

$$E_{s,l,j}(p) = \int d\Omega_{\rm p} \sum_{l_z,s_z}\sum_{l_z',s_z'}\sum_{s_{1,z}}\sum_{s_{2,z}} C_{0,l_z,s_z}^{j,l,s} C_{s_z,s_{1,z},s_{2,z}}^{s,s_1,s_2} C_{0,l_z',s_z'}^{j,l,s} C_{s_z',s_{1,z},s_{2,z}}^{s,s_1,s_2} Y_{l,l_z}^*(\vec{p}/p) Y_{l,l_z'}(\vec{p}/p) E(\vec{p}). \tag{16}$$

The angular integration can be facilitated by Taylor-expanding $E(\vec{p})$ up to order $\mathcal{O}(p^{\kappa})$ which should be sufficiently high to yield accurate results up to the cutoff momentum π/a. [2] Afterwards, the CMS momentum can be computed by solving $E_{s,l,j}(p)$ for p.

D. Scattering with two coupled channels

For two coupled channels, the S-matrix must be constructed as

$$S = \begin{pmatrix} \vec{A}_1^+ & \vec{A}_2^+ \end{pmatrix} \begin{pmatrix} \vec{A}_1^- & \vec{A}_2^- \end{pmatrix}^{-1} \tag{17}$$

where $\vec{A}_1^{\pm}, \vec{A}_2^{\pm}$ are linearly independent two-component vectors containing the coefficients in front of the spherical Hankel functions $h_{l_i}^{\pm}$. A simple way to obtain these coefficients would be to extract them from a complex wave function

$$\vec{\psi}(r) = \begin{pmatrix} A_1 h_{l_1}^-(pr) + B_1 h_{l_1}^+(pr) \\ A_2 h_{l_1}^-(pr) + B_2 h_{l_2}^+(pr) \end{pmatrix} \tag{18}$$

and its complex conjugate

$$\vec{\psi}^*(r) = \begin{pmatrix} A_1^* h_{l_1}^+(pr) + B_1^* h_{l_1}^-(pr) \\ A_2^* h_{l_1}^+(pr) + B_2^* h_{l_2}^-(pr) \end{pmatrix} \tag{19}$$

using

$$\vec{A}_1^- = (A_1, A_2)^{\rm T}, \quad \vec{A}_2^- = (B_1^*, B_2^*)^{\rm T}, \quad \vec{A}_1^+ = (B_1, B_2)^{\rm T}, \quad \vec{A}_2^+ = (A_1^*, A_2^*)^{\rm T}. \tag{20}$$

———————

[2] In numerical calculations, we use $\kappa = 30$.

However, the Hamiltonian H_{r} commutes with the time reversal operator $\mathbb{T}$ so that it holds

$$\vec{\psi}^* = \mathbb{T}\vec{\psi} = \vec{\psi} \quad \Rightarrow \quad \vec{A}_1^{\pm} = \vec{A}_2^{\pm}, \tag{21}$$

i. e. the vectors $\vec{A}_1^{\pm}, \vec{A}_2^{\pm}$ are linearly dependent. Thus, one runs into the problem of having only one independent solution per lattice energy. In order to circumvent this problem, an auxiliary imaginary potential term that breaks the time reversal symmetry can be added to the Hamiltonian:

$$(H_{\mathrm{r}} + U)\vec{\psi}(r) = E\vec{\psi}(r) \tag{22}$$

with

$$U(r) = U_0 \delta_{r,R_{\mathrm{M}}} \begin{pmatrix} 0 & i \\ -i & 0 \end{pmatrix} \tag{23}$$

and $U_0 \in \mathbb{R}$. The radius R_{M} should lie outside the range of the test potential and can be chosen close to the spherical wall radius, $R_{\mathrm{M}} \lesssim R_{\mathrm{W}}$. Because the matrix in Eq. (23) mixes the two channels, $U(r)$ will be referred to as the mixing potential. Finally, the S-matrix is decomposed according to the Blatt-Biedenharn parametrization [53]

$$S = \begin{pmatrix} \cos\epsilon & \sin\epsilon \\ -\sin\epsilon & \cos\epsilon \end{pmatrix}^{-1} \begin{pmatrix} e^{2i\delta_1} & 0 \\ 0 & e^{2i\delta_2} \end{pmatrix} \begin{pmatrix} \cos\epsilon & \sin\epsilon \\ -\sin\epsilon & \cos\epsilon \end{pmatrix} \tag{24}$$

with the phase shifts δ_1, δ_2 and the mixing angle ϵ. Since the lattice dispersion relation can yield slightly different momenta p_1, p_2 for the two channels at the same energy, we assume that the phase shift δ_{α} is measured at momentum p_{α} and that the mixing angle is measured at the average momentum $(p_1 + p_2)/2$.

E. Scattering with an arbitrary number of coupled channels

If $n > 2$ coupled channels must be considered, one needs n linearly independent wave functions in each channel. The complex conjugation is not sufficient for this purpose because it can only generate two independent solutions ψ and ψ^*. In order to find an alternative approach, we first consider the case of two coupled partial waves again. The two-channel wave function $\vec{\psi}(r) = (\psi_1(r), \ \psi_2(r))^T$ can be rewritten as

$$\vec{\psi}'(r) = (\mathrm{Re}\,\psi_1(r), \ \mathrm{Im}\,\psi_1(r), \ \mathrm{Re}\,\psi_2(r), \ \mathrm{Im}\,\psi_2(r))^T. \tag{25}$$

To reproduce Eqs. (22), (23), the radial Hamiltonian and the mixing potential must be modified accordingly:

$$H_{\mathrm{r}}' = \left(\begin{array}{cc|cc} (H_{\mathrm{r}})_{11} & 0 & (H_{\mathrm{r}})_{12} & 0 \\ 0 & (H_{\mathrm{r}})_{11} & 0 & (H_{\mathrm{r}})_{12} \\ \hline (H_{\mathrm{r}})_{21} & 0 & (H_{\mathrm{r}})_{22} & 0 \\ 0 & (H_{\mathrm{r}})_{21} & 0 & (H_{\mathrm{r}})_{22} \end{array} \right), \qquad U' = U_0\, \delta_{r,R_{\mathrm{M}}} \left(\begin{array}{cc|cc} 0 & 0 & 0 & -1 \\ 0 & 0 & 1 & 0 \\ \hline 0 & 1 & 0 & 0 \\ -1 & 0 & 0 & 0 \end{array} \right). \tag{26}$$

On the other hand, instead of using Eq. (25), we can regard the wave function vector as having four independent complex components

$$\vec{\psi}'(r) = (\psi_1'(r), \ \psi_2'(r), \ \psi_3'(r), \ \psi_4'(r))^T. \tag{27}$$

A natural extension of Eqs. (26), (27) to three coupled scattering channels is given by introducing

$$H_{\mathrm{r}}' = \left(\begin{array}{ccc|ccc|ccc} (H_{\mathrm{r}})_{11} & 0 & 0 & (H_{\mathrm{r}})_{12} & 0 & 0 & (H_{\mathrm{r}})_{13} & 0 & 0 \\ 0 & (H_{\mathrm{r}})_{11} & 0 & 0 & (H_{\mathrm{r}})_{12} & 0 & 0 & (H_{\mathrm{r}})_{13} & 0 \\ 0 & 0 & (H_{\mathrm{r}})_{11} & 0 & 0 & (H_{\mathrm{r}})_{12} & 0 & 0 & (H_{\mathrm{r}})_{13} \\ \hline (H_{\mathrm{r}})_{21} & 0 & 0 & (H_{\mathrm{r}})_{22} & 0 & 0 & (H_{\mathrm{r}})_{23} & 0 & 0 \\ 0 & (H_{\mathrm{r}})_{21} & 0 & 0 & (H_{\mathrm{r}})_{22} & 0 & 0 & (H_{\mathrm{r}})_{23} & 0 \\ 0 & 0 & (H_{\mathrm{r}})_{21} & 0 & 0 & (H_{\mathrm{r}})_{22} & 0 & 0 & (H_{\mathrm{r}})_{23} \\ \hline (H_{\mathrm{r}})_{31} & 0 & 0 & (H_{\mathrm{r}})_{32} & 0 & 0 & (H_{\mathrm{r}})_{33} & 0 & 0 \\ 0 & (H_{\mathrm{r}})_{31} & 0 & 0 & (H_{\mathrm{r}})_{32} & 0 & 0 & (H_{\mathrm{r}})_{33} & 0 \\ 0 & 0 & (H_{\mathrm{r}})_{31} & 0 & 0 & (H_{\mathrm{r}})_{32} & 0 & 0 & (H_{\mathrm{r}})_{33} \end{array} \right),$$

$$U' = U_0\,\delta_{r,R_{\mathrm{M}}} \begin{pmatrix} 0 & 0 & 0 & 0 & -1 & 1 & 0 & 1 & -1 \\ 0 & 0 & 0 & 1 & 0 & 1 & 1 & 0 & 1 \\ 0 & 0 & 0 & 1 & 1 & 0 & 1 & 1 & 0 \\ \hline 0 & 1 & 1 & 0 & 0 & 0 & 0 & 1 & 1 \\ -1 & 0 & 1 & 0 & 0 & 0 & 1 & 0 & -1 \\ 1 & 1 & 0 & 0 & 0 & 0 & 1 & 1 & 0 \\ \hline 0 & 1 & 1 & 0 & 1 & 1 & 0 & 0 & 0 \\ 1 & 0 & 1 & 1 & 0 & 1 & 0 & 0 & 0 \\ -1 & 1 & 0 & 1 & -1 & 0 & 0 & 0 & 0 \end{pmatrix}, \quad \vec{\psi}'(r) = \begin{pmatrix} \psi_1'(r) \\ \psi_2'(r) \\ \psi_3'(r) \\ \psi_4'(r) \\ \psi_5'(r) \\ \psi_6'(r) \\ \psi_7'(r) \\ \psi_8'(r) \\ \psi_9'(r) \end{pmatrix}. \tag{28}$$

A generalization to n channels is straightforward:

$$\begin{aligned} (H_{\mathrm{r}}')_{\alpha'+(\alpha-1)n,\beta'+(\beta-1)n} &= (H_{\mathrm{r}})_{\alpha\beta}\delta_{\alpha',\beta'}, \\ U'_{\alpha'+(\alpha-1)n,\beta'+(\beta-1)n} &= U_0\delta_{r,R_{\mathrm{M}}}(1-\delta_{\alpha\beta})(1-\delta_{\alpha'\beta'}-2\delta_{\alpha\alpha'}\delta_{\beta\beta'}) \end{aligned} \tag{29}$$

for $\alpha,\alpha',\beta,\beta' = 1,\dots,n$. The wave function vector has the form

$$\vec{\psi}'(r) = (\psi_1'(r),\dots,\psi_{n^2}'(r))^{\mathrm{T}} \tag{30}$$

where $\psi_{\beta+(\alpha-1)n}'$ denotes the β-th wave function for the α-th scattering channel with $\alpha,\beta = 1,\dots,n$.

More generally, any Hermitian matrix that produces n linearly independent solutions in every channel can be used to define the mixing potential, i. e. it must hold $U'^{\dagger} = U'$ and the matrix M with

$$M_{\alpha,\beta} = \sum_{\alpha',\beta'=1}^{n} (H_{\mathrm{r}}')_{\beta+(\alpha-1)n,\beta'+(\alpha'-1)n}h_{l_{\alpha'}}^{\pm} + \sum_{\alpha',\beta'=1}^{n} U'_{\beta+(\alpha-1)n,\beta'+(\alpha'-1)n}h_{l_{\alpha'}}^{\pm} \tag{31}$$

must have rank n. The particular choice for the mixing potential in Eq. (29) is consistent with the one employed for two channels in Ref. [49].

Each component of the wave function vector has the form

$$\psi_{\beta+(\alpha-1)n}'(r) = A_{\alpha\beta}h_{l_\alpha}^{-}(pr) + B_{\alpha\beta}h_{l_\alpha}^{+}(pr) \tag{32}$$

with $\alpha,\beta = 1,\dots,n$. Since it holds

$$\begin{pmatrix} B_{1\beta} \\ \vdots \\ B_{n\beta} \end{pmatrix} = S \begin{pmatrix} A_{1\beta} \\ \vdots \\ A_{n\beta} \end{pmatrix} \tag{33}$$

for $\beta = 1,\dots,n$, one can construct the S-matrix as

$$S = \begin{pmatrix} B_{11} & \cdots & B_{1n} \\ \vdots & \ddots & \vdots \\ B_{n1} & \cdots & B_{nn} \end{pmatrix} \begin{pmatrix} A_{11} & \cdots & A_{1n} \\ \vdots & \ddots & \vdots \\ A_{n1} & \cdots & A_{nn} \end{pmatrix}^{-1}. \tag{34}$$

The Blatt-Biedenharn parametrization also has to be extended to $n > 2$ coupled channels [53]:

$$S = O^{-1}\mathrm{diag}(e^{2i\delta_1},\dots,e^{2i\delta_n})O \tag{35}$$

where O is a real orthogonal matrix. (This decomposition is equivalent to computing the eigenvalues and eigenvectors of S.) Again, the phase shift δ_α is assigned to the momentum p_α in scattering channel α. For simplicity, we define the mixing angles as

$$\epsilon_{\alpha\beta}\left(p = \frac{p_\alpha + p_\beta}{2}\right) = \tan^{-1} O_{\alpha\beta} \tag{36}$$

for $\alpha,\beta = 1,\dots,n$ and $\beta > \alpha$ because a real orthogonal $n \times n$-matrix is uniquely given by $n(n-1)/2$ real parameters.

n_{ch}	L [a]	R_{I} [a]	R_{O} [a]	R_{W} [a]	V_0 [MeV]	U_0 [MeV]	n_{eigs}
1	35	9.02	12.02	15.02	0	—	10
	41	9.02	12.02	18.02	0	—	10
	47	9.02	12.02	21.02	0	—	10
2	35	9.02	12.02	15.02	0	20	15
	41	9.02	12.02	18.02	0	20	15
3	35	9.02	12.02	15.02	0	10	70
4	35	9.02	12.02	15.02	0	5	110

TABLE I: Parameters for the lattice calculation depending on the number of coupled scattering channels (n_{ch}): lattice length L, interval $[R_{\mathrm{I}}, R_{\mathrm{O}}]$ for fitting wave functions, spherical wall radius R_{W}, coefficient V_0 of Gaussian auxiliary potential, coefficient U_0 of mixing potential and number of computed eigenvectors n_{eigs}. The lattice spacing has been chosen as $a = 1.9733$ fm.

III.   TEST CASE: SCATTERING OF TWO SPIN-1 PARTICLES

The method described in section II allows one to determine scattering phase shifts and mixing angles on the lattice for an arbitrary number of coupled channels and for any type of particles. As a concrete example, we consider the scattering problem of two spin-1 bosons having nearly the same mass as the deuteron, $m_{1,2} = 2m_{\mathrm{N}} = 2 \times 938.92$ MeV. As a test potential, we employ the corresponding generalization of the toy-model potential used for two spin-1/2 fermions in Refs. [48, 49]:

$$V(\vec{r}) = C \left(1 + \frac{s_{12}(\vec{r})}{r_0^2}\right) \exp\left(-\frac{r^2}{2r_0^2}\right) \tag{1}$$

where the spin-dependent part is given by

$$s_{12}(\vec{r}) = 3(\vec{r} \cdot \vec{s}_1)(\vec{r} \cdot \vec{s}_2) - (\vec{s}_1 \cdot \vec{s}_2)r^2. \tag{2}$$

Here, $\vec{s}_1$ and $\vec{s}_2$ denote the spin matrices for the considered particles. The constants are set to $C = -2$ MeV and $r_0 = 0.02$ MeV^{-1}, and the lattice spacing is chosen to be $a = (100 \text{ MeV})^{-1} = 1.9733$ fm. Notice that by projecting the test potential onto partial waves one obtains up to four coupled scattering channels. We calculate the phase shifts and mixing angles for the following cases:

- Uncoupled channels: $^3\mathrm{P}_0$, $^3\mathrm{P}_1$, $^3\mathrm{D}_2$, $^3\mathrm{F}_3$, $^3\mathrm{G}_4$, $^3\mathrm{H}_5$, $^5\mathrm{D}_1$.

- Two coupled channels: $^3\mathrm{SD}_1$, $^3\mathrm{PF}_2$, $^3\mathrm{DG}_3$, $^3\mathrm{FH}_4$, $^1\mathrm{S}_0/^5\mathrm{D}_0$, $^5\mathrm{PF}_2$, $^5\mathrm{DG}_3$, $^5\mathrm{FH}_4$.

- Three coupled channels: $^1\mathrm{P}_1/^5\mathrm{PF}_1$.

- Four coupled channels: $^1\mathrm{D}_2/^5\mathrm{SDG}_2$.

We further emphasize that the considered potential possesses four bound states in the $^3\mathrm{SD}_1$, $^1\mathrm{S}_0/^5\mathrm{D}_0$, $^5\mathrm{PF}_2$ and $^1\mathrm{D}_2/^5\mathrm{SDG}_2$ channels with the binding energies of -0.258 MeV, -0.204 MeV, -0.198 MeV and -0.583 MeV, respectively, as visualized in the right panel of Fig. 1. The binding energies have been obtained by computing the eigenvalues of the momentum-space Hamiltonian in the infinite-volume continuum.

On the lattice, the eigenvectors of the Hamiltonian corresponding to the lowest positive eigenenergies have been used as radial wave functions. The parameters used in our calculations, which have partly been adopted from Ref. [49], can be found in table I while Fig. 1 visualizes the different contributions to the potential on the lattice. Notice that the Gaussian auxiliary potential can distort the wave function and may even generate additional bound states, see Fig. 2. This may result in the appearance of the outlying points in the calculated phase shifts or mixing angles as will be discussed below. For this reason, instead of imposing the auxiliary potential, we have actually varied the lattice size to generate data at low momenta.

The choice of the mixing potential requires some care, too. In particular, as shown in table I, the numerical value of the strength U_0 has been decreased for three and four channels in order to avoid the appearance of additional bound
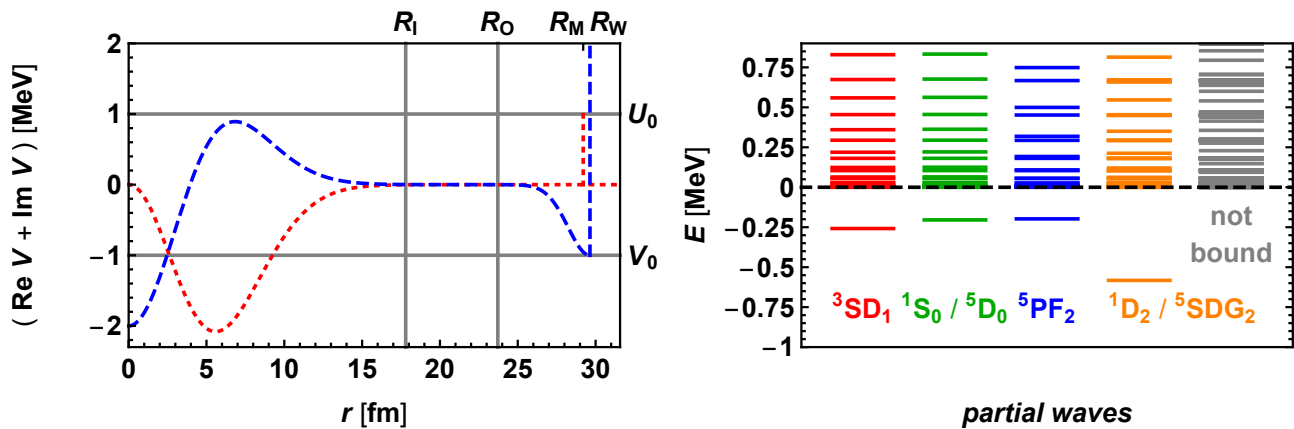
FIG. 1: Left panel (adopted from Ref. [49]): The employed potentials in the $^3SD_1$ partial waves. The blue dashed and red dotted lines show the diagonal $^3D_1$-wave element and the off-diagonal $^3SD_1$-wave element in the 2×2 potential matrix, respectively. V_0 and U_0 give the strengths of the auxiliary and mixing potentials, respectively, R_M shows an approximate position of the mixing potential while R_W is the spherical wall radius. The wave function is fitted in the interval $[R_I, R_O]$. Right panel: Spectrum of eigenenergies in the continuum for different partial waves. The last column shows the combined spectrum in all channels which do not have bound states.
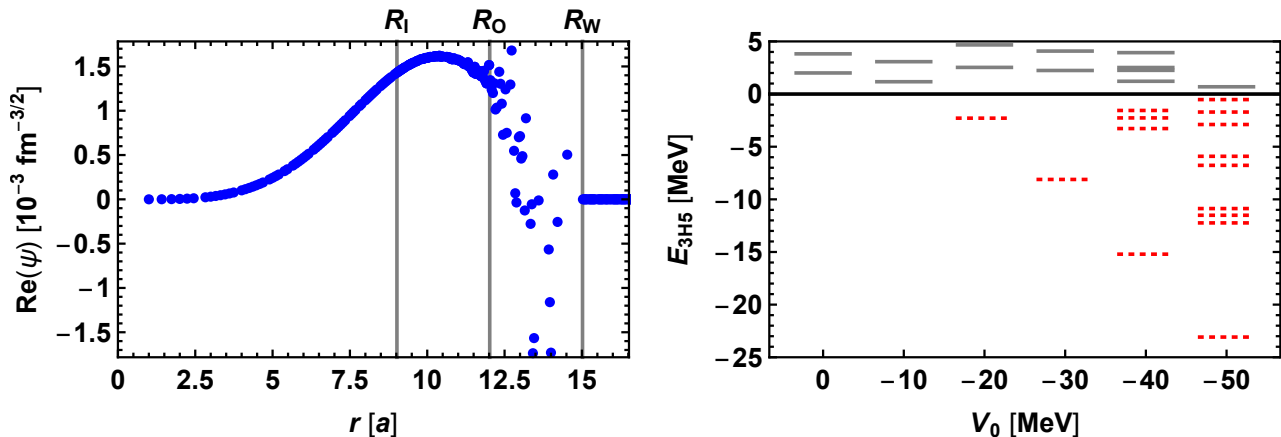
FIG. 2: Effects of the Gaussian auxiliary potential. Left panel: wave function in the $^3H_5$ partial wave distorted by the auxiliary potential of the strength $V_0 = -40$ MeV, which corresponds to the outlying data point at $p \approx 65$ MeV in the last plot in Fig. 4. Right panel: eigenenergies on the lattice in the $^3H_5$ partial wave as functions of the strength V_0 of the auxiliary potential. Large negative values of V_0 lead to additional bound states shown as red dotted lines.

states as visualized in the right panel of Fig. 3. On the other hand, choosing too small in magnitude values of U_0 leads to numerical instabilities causing a violation of unitarity in the calculated S-matrix, see the left panel of Fig. 3.

In Figs. 4−8, we show the phase shifts and mixing angles for all considered scattering channels, which have been calculated on the lattice using the method presented above. To benchmark our calculations, we have also computed the scattering parameters in the continuum. This has been achieved by solving the radial Schrödinger equation for a fixed energy $E = p^2/(2\mu)$. The boundary conditions at $r \approx 0$ have to be chosen in such a way that one obtains a sufficient number of linearly independent solutions. Finally, the S-matrix can again be extracted from the wave function by fitting spherical Hankel functions. As shown in Figs. 4−8, the results of the lattice calculations are in essentially a perfect agreement with the ones calculated using the continuum approach in the considered range of CMS momenta up to $p = 120$ MeV. The cutoff momentum associated with the lattice spacing of $a = (100 \text{ MeV})^{-1} = 1.9733$ fm employed in our analysis is $\Lambda_{latt} \sim \pi/a \simeq 314$ MeV. Thus, the lattice and continuum results are expected to agree for momenta well below Λ_{latt}. Indeed, for CMS momenta higher than $p = 120$ MeV, the deviations between the continuum and lattice results start to become visible. This observation is in line with the findings of Refs. [48, 49].
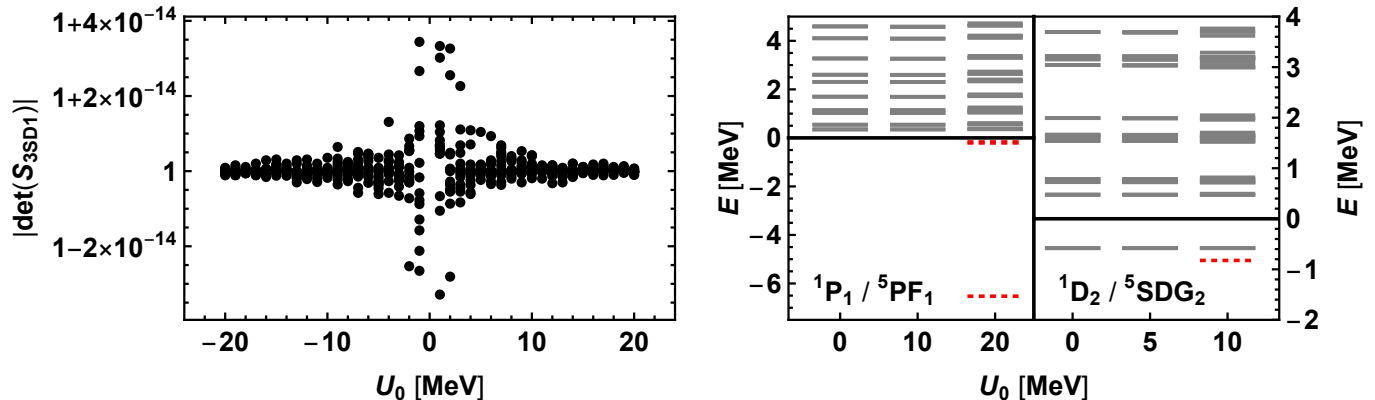
FIG. 3: Effects of the mixing potential. Left panel: absolute values of the determinant of the S-matrix for all eigenenergies in the $^3\text{SD}_1$ partial wave as functions of the strength U_0 of the mixing potential. Small in magnitude values of U_0 lead to numerical instabilities resulting in a non-unitary S-matrix, i. e. $|\det S| \neq 1$. Right panel: eigenenergies on the lattice in the $^1\text{P}_1/^5\text{PF}_1$ ($^1\text{D}_2/^5\text{SDG}_2$) partial waves for the choices of $U_0 = 0$, 10 and 20 MeV ($U_0 = 0$, 5 and 10 MeV). Large values of the strength U_0 of the mixing potential cause the appearance of additional bound states shown by red dotted lines.

We also notice a subtlety in the extraction of phase shifts in multi-channel cases due to the fact that the eigenvalues $e^{2i\delta_1}, \ldots, e^{2i\delta_n}$ of the S-matrix have no pre-defined ordering [53]. Therefore, the multi-channel continuum calculation has been repeated without the off-diagonal elements in the potential matrix, see the gray dashed lines in Figs. 5−8. Then, the phase shifts in the coupled channels have been ordered such that they are roughly consistent with the phase shifts obtained without the coupling. The large differences between the solid and dashed lines demonstrate the very important role of channel mixing in the considered toy model. For many-body systems where no continuum calculation is possible, the comparison can be performed with lattice data instead. If the results at very low momenta are available, one may also possibly identify the partial waves from the threshold behavior of the eigenphases. Last but not least, we emphasize that the behavior the phase shifts in the $^3\text{SD}_1$, $^1\text{S}_0/^5\text{D}_0$, $^5\text{PF}_2$ and $^1\text{D}_2/^5\text{SDG}_2$ channels with $\delta(p = 0) = \pi$ is consistent with the appearance of a single bound state in each of these channels, see the right panel of Fig. 1, in agreement with Levinson's theorem.

IV. SUMMARY AND OUTLOOK

In this paper, we considered two-particle scattering on the lattice. A generalization of the method used in Ref. [49] for spin-1/2 fermions to scattering of particles with any spin and an arbitrary number of coupled scattering channels has been proposed. For the case of two spin-1 bosons, the proposed method was benchmarked against the continuum approach and demonstrated to yield accurate and reliable results for phase shifts and mixing angles for momenta well below the lattice cutoff. Our study opens the way to perform *ab initio* chiral EFT calculations in the four-nucleon continuum and to access nuclear reactions on the lattice using the adiabatic projection method. Work along these lines is in progress.
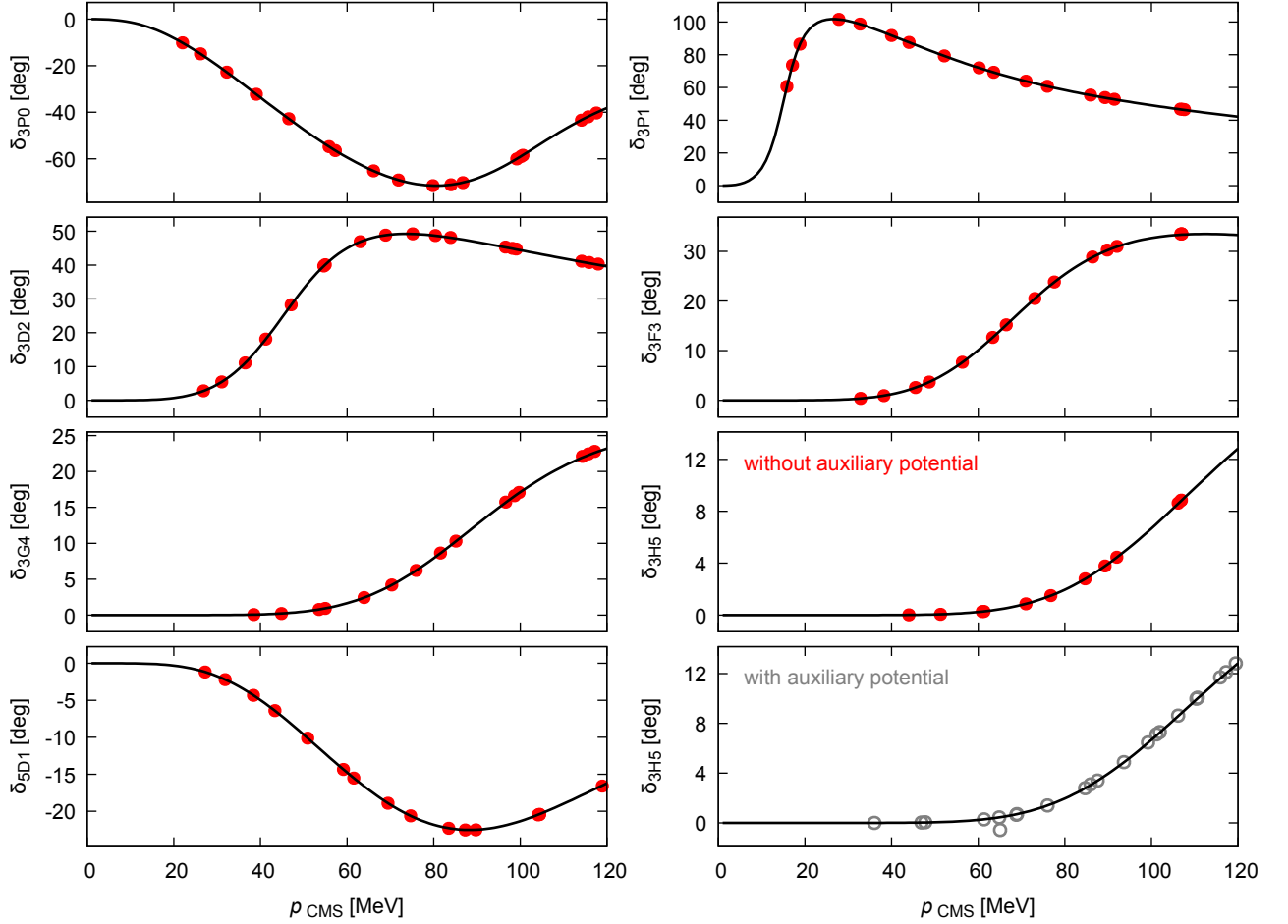
Acknowledgments

FIG. 4: Phase shifts in the uncoupled channels (black solid line: continuum; red points and gray circles: lattice). The last plot shows the $^3H_5$-wave phase shift obtained for the auxiliary potential with $V_0 = 0$ MeV, -10 MeV, ..., -50 MeV at the lattice length $L = 35a$. The outlying data point at $p \approx 65$ MeV corresponds to the value of $V_0 = -40$ MeV.

manuscript. We also thank Ning Li for sharing his nucleon-nucleon scattering code.

[1] M. Tanabashi *et al.* [Particle Data Group], Phys. Rev. D **98**, no. 3, 030001 (2018).
[2] H. W. Hammer, J. Y. Pang and A. Rusetsky, JHEP **1709**, 109 (2017) [arXiv:1706.07700 [hep-lat]].
[3] H.-W. Hammer, J.-Y. Pang and A. Rusetsky, JHEP **1710**, 115 (2017) [arXiv:1707.02176 [hep-lat]].
[4] R. A. Briceno, M. T. Hansen and S. R. Sharpe, Phys. Rev. D **95**, no. 7, 074510 (2017) [arXiv:1701.07465 [hep-lat]].
[5] R. A. Briceno, J. J. Dudek and R. D. Young, Rev. Mod. Phys. **90**, no. 2, 025001 (2018) [arXiv:1706.06223 [hep-lat]].
[6] E. Epelbaum, H. Krebs and U.-G. Meißner, Eur. Phys. J. A **51**, no. 5, 53 (2015) [arXiv:1412.0142 [nucl-th]].
[7] E. Epelbaum, H. Krebs and U.-G. Meißner, Phys. Rev. Lett. **115**, no. 12, 122301 (2015) [arXiv:1412.4623 [nucl-th]].
[8] D. R. Entem, N. Kaiser, R. Machleidt and Y. Nosyk, Phys. Rev. C **91**, no. 1, 014002 (2015) [arXiv:1411.5335 [nucl-th]].
[9] D. R. Entem, R. Machleidt and Y. Nosyk, Phys. Rev. C **96**, no. 2, 024004 (2017) [arXiv:1703.05454 [nucl-th]].
[10] P. Reinert, H. Krebs and E. Epelbaum, Eur. Phys. J. A **54**, no. 5, 86 (2018) [arXiv:1711.08821 [nucl-th]].
[11] S. Ishikawa and M. R. Robilotta, Phys. Rev. C **76**, 014006 (2007) [arXiv:0704.0711 [nucl-th]].
[12] V. Bernard, E. Epelbaum, H. Krebs and U.-G. Meißner, Phys. Rev. C **77**, 064004 (2008) [arXiv:0712.1967 [nucl-th]].
[13] V. Bernard, E. Epelbaum, H. Krebs and U.-G. Meißner, Phys. Rev. C **84**, 054001 (2011) [arXiv:1108.3816 [nucl-th]].
[14] E. Epelbaum, Eur. Phys. J. A **34**, 197 (2007) [arXiv:0710.4250 [nucl-th]].
[15] H. Krebs, A. Gasparyan and E. Epelbaum, Phys. Rev. C **85**, 054006 (2012) [arXiv:1203.0067 [nucl-th]].
[16] H. Krebs, A. Gasparyan and E. Epelbaum, Phys. Rev. C **87**, no. 5, 054007 (2013) [arXiv:1302.2872 [nucl-th]].
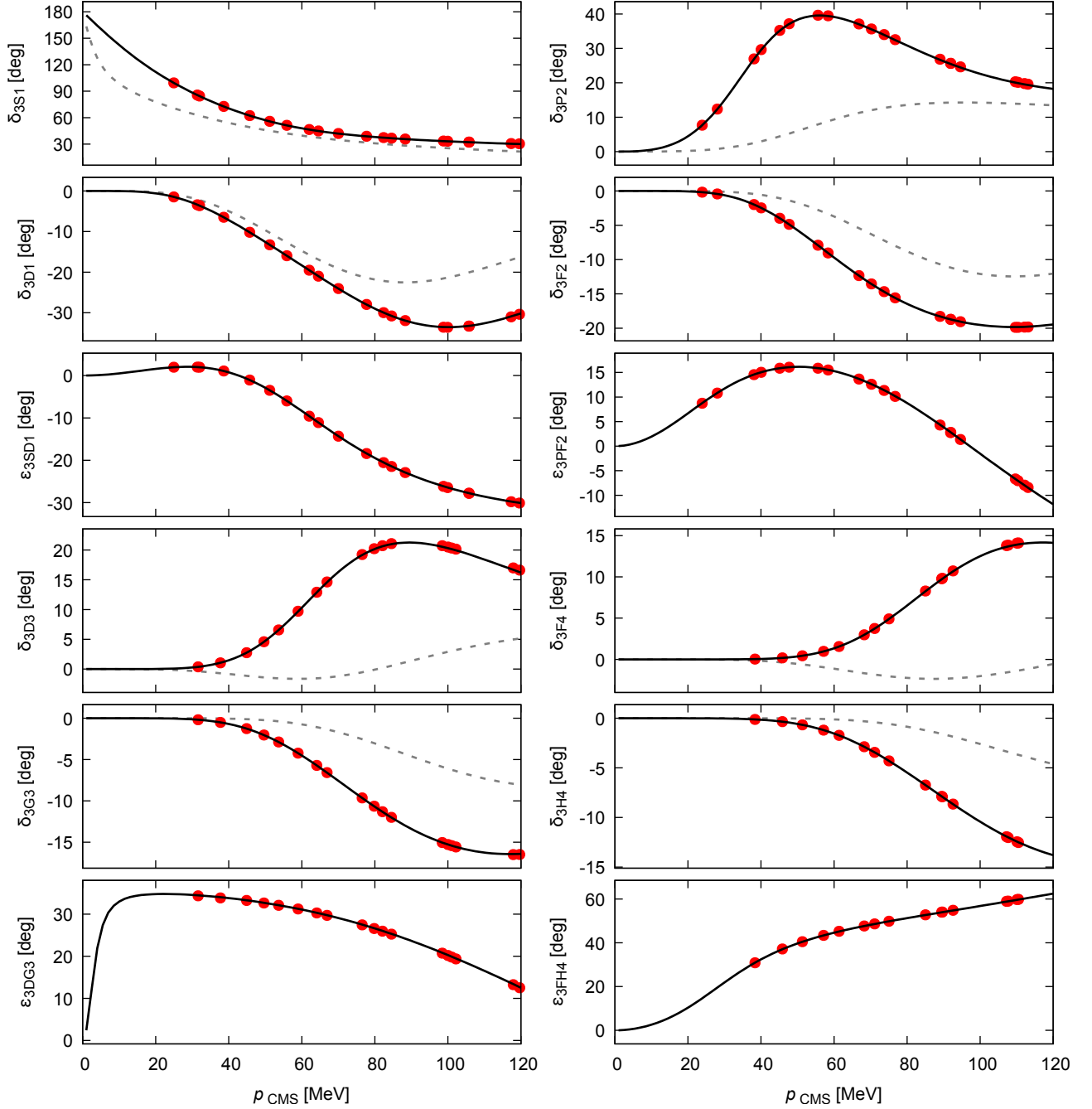
FIG. 5: Phase shifts and mixing angles in the pairs of coupled channels for spin $s = 1$ (black solid line: continuum; red points: lattice; gray dashed line: continuum results without channel mixing).

[17] E. Epelbaum, A. M. Gasparyan, H. Krebs and C. Schat, Eur. Phys. J. A **51**, no. 3, 26 (2015) [arXiv:1411.3612 [nucl-th]].
[18] L. Girlanda, A. Kievsky and M. Viviani, Phys. Rev. C **84**, 014001 (2011) [arXiv:1102.4799 [nucl-th]].
[19] E. Epelbaum, H. W. Hammer and U.-G. Meißner, Rev. Mod. Phys. **81**, 1773 (2009) [arXiv:0811.1338 [nucl-th]].
[20] E. Epelbaum and U.-G. Meißner, Ann. Rev. Nucl. Part. Sci. **62**, 159 (2012) [arXiv:1201.2136 [nucl-th]].
[21] R. Machleidt and D. R. Entem, Phys. Rept. **503**, 1 (2011) [arXiv:1105.2919 [nucl-th]].
[22] W. Glöckle, H. Witala, D. Huber, H. Kamada and J. Golak, Phys. Rept. **274**, 107 (1996).
[23] B. R. Barrett, P. Navratil and J. P. Vary, Prog. Part. Nucl. Phys. **69**, 131 (2013).
[24] G. Hagen, M. Hjorth-Jensen, G. R. Jansen, R. Machleidt and T. Papenbrock, Phys. Rev. Lett. **109**, 032502 (2012) [arXiv:1204.3612 [nucl-th]].
[25] H. Hergert, S. K. Bogner, S. Binder, A. Calci, J. Langhammer, R. Roth and A. Schwenk, Phys. Rev. C **87**, no. 3, 034307
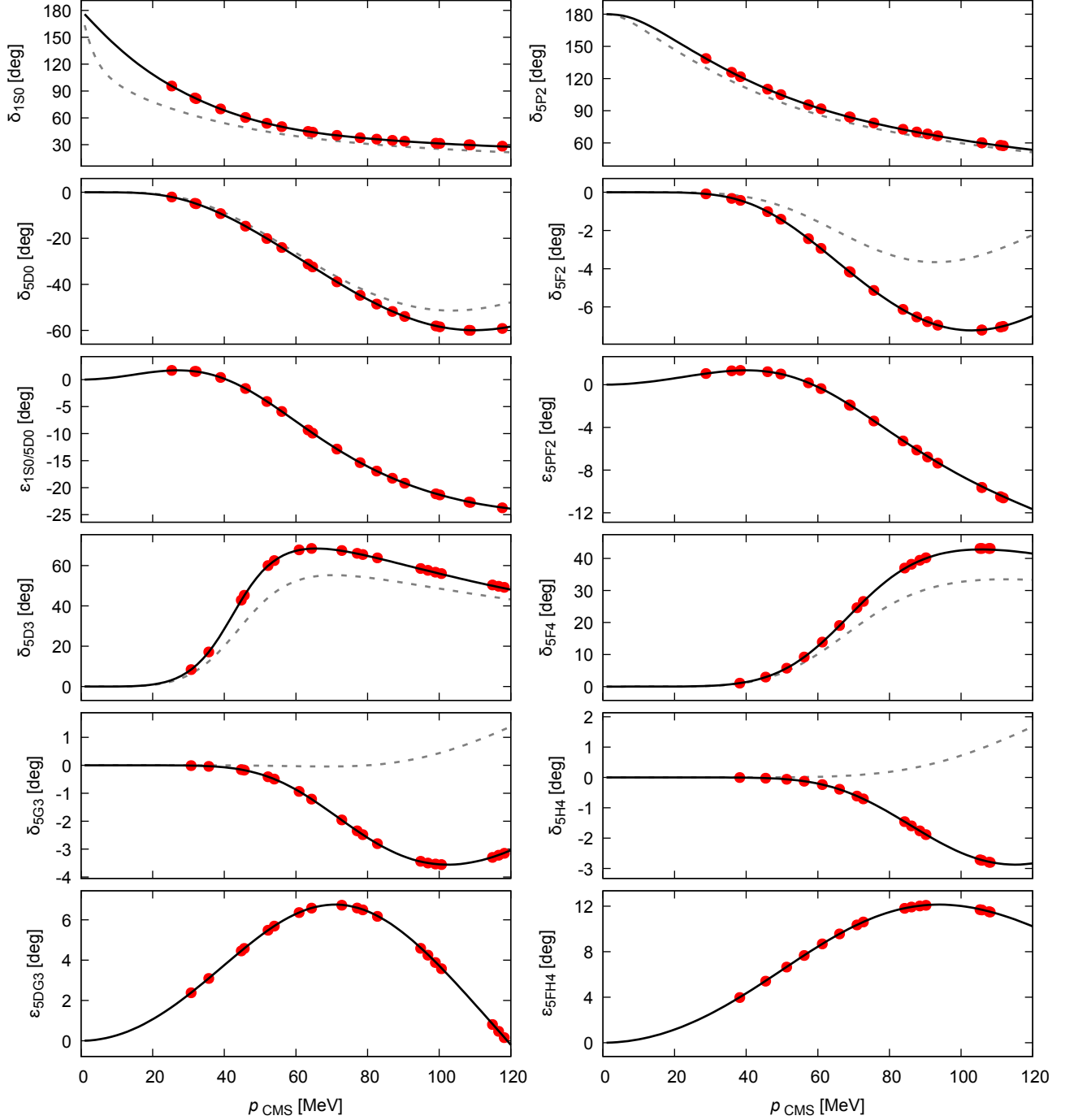
FIG. 6: Phase shifts and mixing angles in the pairs of coupled channels for spin $s = 0, 2$ (black solid line: continuum; red points: lattice; gray dashed line: continuum results without channel mixing).

(2013) [arXiv:1212.1190 [nucl-th]].

[26] V. Soma, C. Barbieri and T. Duguet, Phys. Rev. C **87**, no. 1, 011303 (2013) [arXiv:1208.2472 [nucl-th]].

[27] A. Lovato, S. Gandolfi, R. Butler, J. Carlson, E. Lusk, S. C. Pieper and R. Schiavilla, Phys. Rev. Lett. **111**, no. 9, 092501 (2013) [arXiv:1305.6959 [nucl-th]].

[28] D. Lee, Prog. Part. Nucl. Phys. **63**, 117 (2009) [arXiv:0804.3501 [nucl-th]].

[29] D. Lee, Lect. Notes Phys. **936**, 237 (2017) [arXiv:1609.00421 [nucl-th]].

[30] T. A. Lähde and U.-G. Meißner, Lect. Notes. Phys. **957**, 1 (2019).

[31] E. Epelbaum, H. Krebs, D. Lee and U.-G. Meißner, Phys. Rev. Lett. **106**, 192501 (2011) [arXiv:1101.2547 [nucl-th]].
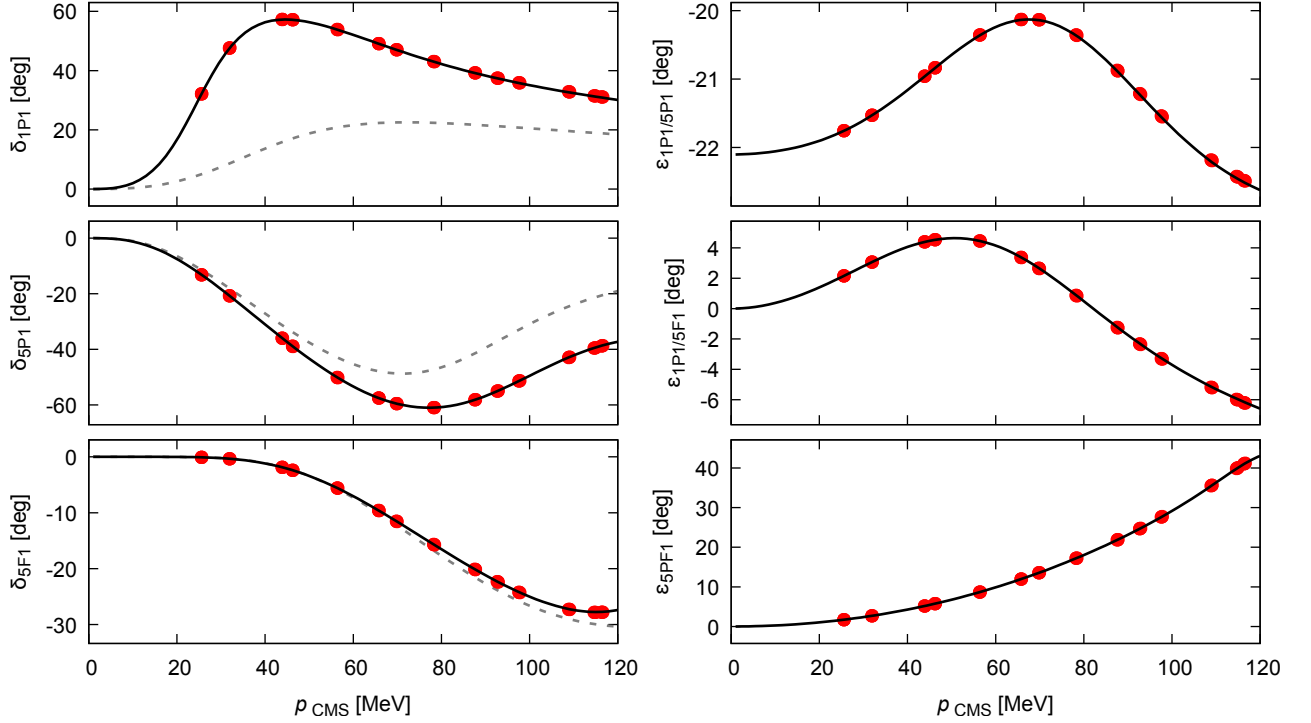
FIG. 7: Phase shifts and mixing angles for the $^1P_1/^5PF_1$-wave (black solid line: continuum; red points: lattice; gray dashed line: continuum results without channel mixing).

[32] E. Epelbaum, H. Krebs, T. A. Lähde, D. Lee and U.-G. Meißner, Phys. Rev. Lett. **109**, 252501 (2012) [arXiv:1208.1328 [nucl-th]].
[33] E. Epelbaum, H. Krebs, T. A. Lähde, D. Lee, U.-G. Meißner and G. Rupak, Phys. Rev. Lett. **112**, no. 10, 102501 (2014) [arXiv:1312.7703 [nucl-th]].
[34] M. Freer, H. Horiuchi, Y. Kanada-En'yo, D. Lee and U.-G. Meißner, Rev. Mod. Phys. **90**, no. 3, 035004 (2018) [arXiv:1705.06192 [nucl-th]].
[35] B. Borasoy, E. Epelbaum, H. Krebs, D. Lee and U.-G. Meißner, Eur. Phys. J. A **35**, 357 (2008) [arXiv:0712.2993 [nucl-th]].
[36] E. Epelbaum, H. Krebs, D. Lee and U.-G. Meißner, Eur. Phys. J. A **41**, 125 (2009) [arXiv:0903.1666 [nucl-th]].
[37] T. A. Lähde, E. Epelbaum, H. Krebs, D. Lee, U.-G. Meißner and G. Rupak, Phys. Lett. B **732**, 110 (2014) [arXiv:1311.0477 [nucl-th]].
[38] N. Li, S. Elhatisari, E. Epelbaum, D. Lee, B. N. Lu and U.-G. Meißner, Phys. Rev. C **98**, no. 4, 044002 (2018) [arXiv:1806.07994 [nucl-th]].
[39] E. Epelbaum, H. Krebs, T. A. Lähde, D. Lee and U.-G. Meißner, Phys. Rev. Lett. **110**, no. 11, 112502 (2013) [arXiv:1212.4181 [nucl-th]].
[40] E. Epelbaum, H. Krebs, T. A. Lähde, D. Lee and U.-G. Meißner, Eur. Phys. J. A **49**, 82 (2013) [arXiv:1303.4856 [nucl-th]].
[41] U.-G. Meißner, Sci. Bull. **60**, no. 1, 43 (2015) [arXiv:1409.2959 [hep-th]].
[42] S. Elhatisari *et al.*, Phys. Rev. Lett. **119**, no. 22, 222505 (2017) [arXiv:1702.05177 [nucl-th]].
[43] B. N. Lu, N. Li, S. Elhatisari, D. Lee, E. Epelbaum and U.-G. Meißner, arXiv:1812.10928 [nucl-th].
[44] J. M. Alarcon *et al.*, Eur. Phys. J. A **53**, no. 5, 83 (2017) [arXiv:1702.05319 [nucl-th]].
[45] N. Klein, D. Lee and U.-G. Meißner, Eur. Phys. J. A **54**, no. 12, 233 (2018) [arXiv:1807.04234 [hep-lat]].
[46] N. Li, S. Elhatisari, E. Epelbaum, D. Lee, B. N. Lu and U.-G. Meißner, arXiv:1902.01295 [nucl-th].
[47] J. Carlson, V. R. Pandharipande and R. B. Wiringa, Nucl. Phys. A **424**, 47 (1984).
[48] B. Borasoy, E. Epelbaum, H. Krebs, D. Lee and U.-G. Meißner, Eur. Phys. J. A **34**, 185 (2007) [arXiv:0708.1780 [nucl-th]].
[49] B. N. Lu, T. A. Lähde, D. Lee and U.-G. Meißner, Phys. Lett. B **760**, 309 (2016) [arXiv:1506.05652 [nucl-th]].
[50] A. Rokash, M. Pine, S. Elhatisari, D. Lee, E. Epelbaum and H. Krebs, Phys. Rev. C **92**, no. 5, 054612 (2015) [arXiv:1505.02967 [nucl-th]].
[51] S. Elhatisari, D. Lee, U.-G. Meißner and G. Rupak, Eur. Phys. J. A **52**, no. 6, 174 (2016) [arXiv:1603.02333 [nucl-th]].
[52] S. Elhatisari, D. Lee, G. Rupak, E. Epelbaum, H. Krebs, T. A. Lähde, T. Luu and U.-G. Meißner, Nature **528**, 111 (2015) [arXiv:1506.03513 [nucl-th]].
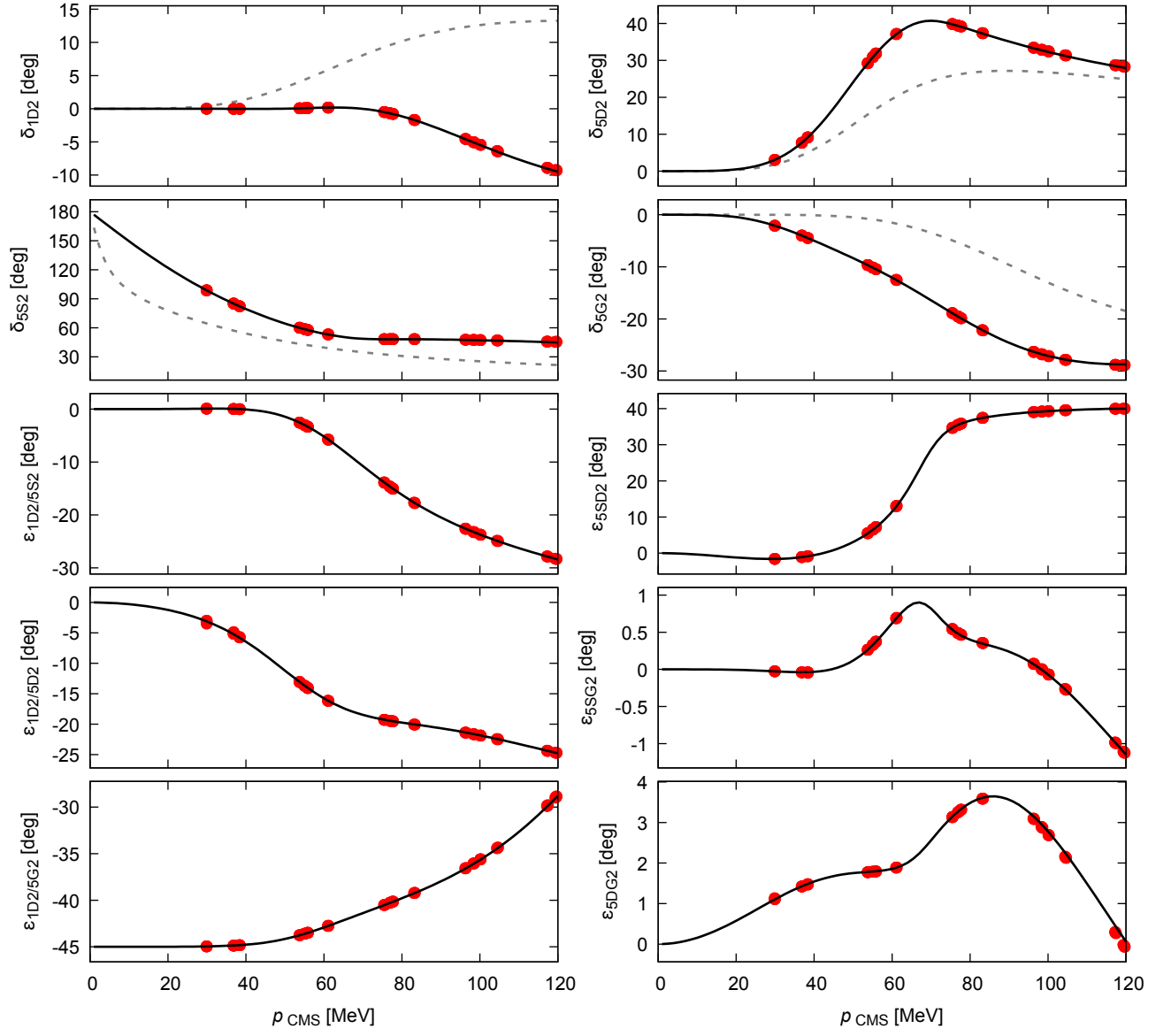[53] J. M. Blatt and L. C. Biedenharn, Phys. Rev. **86**, 399 (1952).

FIG. 8: Phase shifts and mixing angles for the $^1D_2/^5SDG_2$-wave (black solid line: continuum; red points: lattice; gray dashed line: continuum results without channel mixing).